NUCLEAR THEORY, Vol. 37 (2018)
eds. M. Gaidarov, N. Minkov, Heron Press, Sofia

$j-1$ Anomaly Across the Shells

Stefan Lalkovski

Department of Nuclear Engineering, Faculty of Physics,
"St. Kl. Ohridski" University of Sofia

Abstract. The Nuclear Shell model and the Particle – Deformed Core models are two of the main paradigmata in modern Nuclear physics. Their success in describing low-energy features of atomic nuclei is guaranteed by the adiabatic principle which allows to disentangle single-particle from collective excitation modes. As a consequence, the nuclei with well pronounced shell-model behaviour are clustered around the magic numbers on the Segré chart, while nuclei with large number of valence particles form regions of collectivity, placed in between the magic gaps. In practice, however, spherical states can be found in a region of deformed nuclei and vice versa. Further, some features typical for one or the other excitation mode seems to gradually change with the valence number from closed shells to the respective mid-shell regions and vice versa. Thus, for example, the seniority consept naturally arises from the spherical shell model, but it is completely "orthogonal" to the deformed shell model approach. Still, recent data shows that seniority states seems to gradually evolve into deformed states when moving away from the magic numbers, suggesting that some of the spherical shell model features survive in the mass regions of well developed collectivity.

1 Introduction

The Nuclear Shell model [1] was introduced in the mid 20th century and become one of the cornerstones in the contemporary nuclear physics owing to its success, among others, in describing the nuclear "magic" numbers. It is now well established that these magic numbers emerge due to the spin-orbit force [2, 3] which, at the medium-mass and heavy nuclei, decouples single-particle orbits from the upper shells and pushes them down in energy to the shells where the majority of the single-particle states have parities opposite to that of the "intruder" states. This phenomenon is responsible for the magic gaps formation at occupation numbers 28, 50, 82 and 126, but also for the emergence of some sub-shell gaps, at $Z = 40$ for example, where extra stability towards nuclear excitations is observed. The respective single-particle orbits that take part in the shells re-arrangement are $f_{7/2}$, $g_{9/2}$, $h_{11/2}$ and $i_{13/2}$.

It worth noting that the Nuclear shell model has been developed and parametrized with respect to the nuclei placed on, or close, to the line of β stability. Some recent experiments, however, suggest that the spin-orbit interaction might weaken, or even vanish, in the regions away of that line.

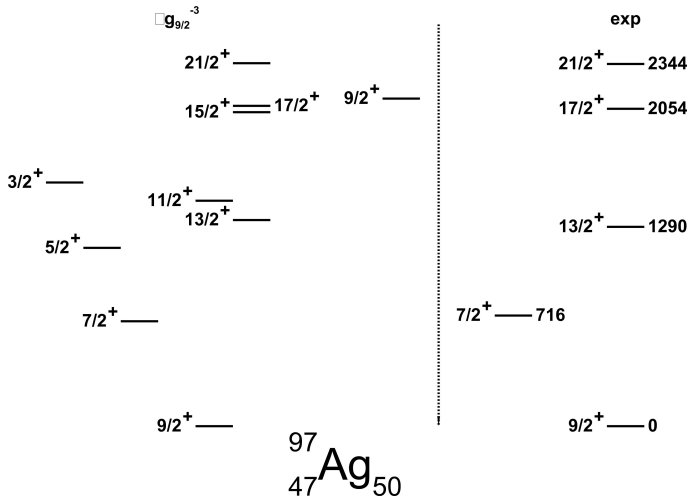

Figure 1. Experimental and theoretical level energies of $^{97}_{47}\mathrm{Ag}_{66}$.

However, already at the line of β stability, the spin-orbit interaction strength varies from shell to shell, and differs for protons and neutrons. The net result is a slightly different ordering of the single particle levels [3, 4], depending on the mass region and the type of nucleons considered. Given that $\pi g_{9/2}$ is the only positive-parity orbit below the $Z = 50$ magic number, and that it is also responsible for the appearance of the sub-shell closure at $Z = 40$, it is natural to expect that this particular orbit plays a major role in the wave-functions of the positive-parity low-ling states in the Ag nuclei. Indeed, as shown in Figure. 1, the lowest-lying positive-parity state observed in $^{97}_{47}\mathrm{Ag}_{50}$ is $9/2^+$, which can be associated with $\pi g_{9/2}$ occupation. The next excited positive-parity state is $7/2^+$, which to certain extent fits to single-particle picture, given that it could arise from excitations across the $Z = 50$ shell gap, and hence can be associated with an occupation of the $\pi g_{7/2}$ orbit. However, the shell gap at $Z = 50$ is about 4 MeV wide. In contrast, the experimental $7/2^+$ state appears to be too low in energy. In the medium-mass silver nuclei the ordering of these two levels is even more tantalizing. There, as shown in Figure 2, $7/2^+$ becomes the lowest-lying positive-parity state. This effect is now known as the $j-1$ anomaly.

2 j^{-3} Coupling Scheme

The idea of $7/2^+$ being a single-particle excitation was abandoned as early, as in the 1960s. At that time the experimental level energies of the most exotic neutron deficient silver nucleus ^{97}Ag were unknown, but the $7/2^+, 9/2^+$ doublet re-ordering was already observed in the neutron mid-shell silver isotopes rising questions about the nature of the anomaly. In the 1960s, Kisslinger pointed

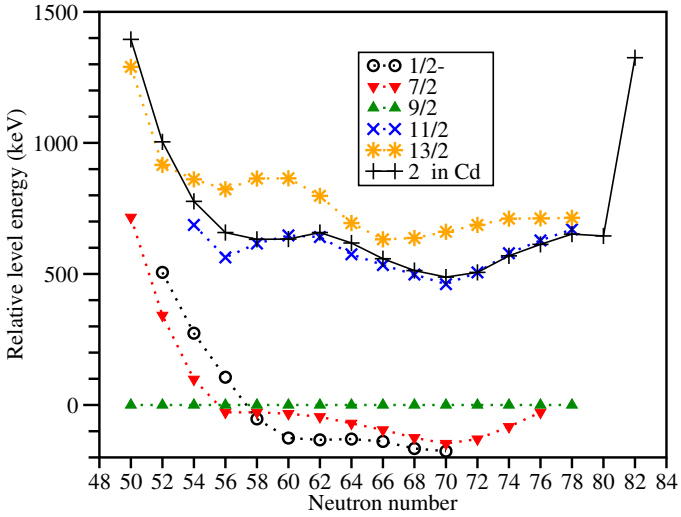

Figure 2. Yrast states in Ag nuclei as a function of the neutron number. All level energies are relative to the $9/2^+$ level. Modified from [5], including new data from [6] and [18].

out [8] that in such nuclei the anomalous ordering of j and $j-1$ levels can be generated by three particle/hole single-j clusters.

The j^{-3} scheme is a direct derivative from the Nuclear shell model. The split seniority scheme arises from the residual interaction between the valence particles, and the maximum spin that can be generated depends on the single-particle orbit. In the case of $g_{9/2}^{-3}$ configuration, the spectrum consists of states with angular momenta $J^\pi = 3/2^+$ to $21/2^+$. All states, except for $9/2_1^+$ state which is seniority $v = 1$ state, are $v = 3$ states [9]. The j^{-3} spectrum [4] can be calculated from the two-body matrix elements $A_{J'}$ as

$$< j^3\alpha; JM|H|j^3\alpha; JM >= 3\sum_{J'}[j^2(J')jJ|\}j^3J]^2 A_{J'}, \qquad (1)$$

where $[j^2(J')jJ|\}j^3J]$ are the coefficients of fractional parentage (cfp). Here j denotes the single-particle total angular momentum; J' is the spin to which two of the particles couple; and J is the total three-particle angular momentum. Table 1 shows the cfp's for three particles on $j = 9/2$ [9].

A way to calculated the j^{-3} spectrum is by using the Talmi procedure, where the two-body matrix elements are determined from the neighbouring even-even semi-magic nucleus having two valence particles or holes. This procedure was used to calculate ^{97}Ag level energies. Two-body matrix elements $A_{J'} = \{0,$ 1395, 2082, 2280, 2428$\}$ keV, were taken from $^{98}_{48}$Cd$_{50}$ assuming that the yrast states are of pure $\pi g_{9/2}^{-2}$ nature. Calculated spectrum is shown in Figure 1 (left hand side). The ordering of $9/2^+$ and $7/2^+$ levels, as well as the energy gap, are

Table 1. Coefficients of fractional parentage for $j = 9/2$ [9, 10]

J	v	$J'=0$	$J'=2$	$J'=4$	$J'=6$	$J'=8$
3/2	3	–	–	2.18182	0.81818	–
5/2	3	–	0.83333	0.59091	1.57576	–
7/2	3	–	1.57576	0.41958	0.00606	0.99860
9/2	1	0.8	0.25	0.45	0.65	0.85
9/2	3	–	0.09848	1.28497	1.45606	0.16049
11/2	3	–	0.51515	1.18881	0.33939	0.95664
13/2	3	–	0.90909	0.18881	0.77273	1.12937
15/2	3	–	–	0.3986	1.90909	0.69231
17/2	3	–	–	0.87413	0.51818	1.60769
21/2	3	–	–	–	0.7	2.3

correctly reproduced. The higher-lying $13/2^+, 17/2^+$ and $21/2^+$ yrast states appear also as they were experimentally observed in Ref. [11]. The $J^\pi = 3/2^+$ and $5/2^+$ states are non-yrast and should appear at higher energies, but they are not observed yet. The $11/2^+$, $15/2^+$ and the $v = 3$, $9/2^+_2$ states are also unknown. Even though some states are not observed yet, the available experimental data on ^{97}Ag is consistent with the j^{-3} coupling scheme.

Alternatively, the two-body matrix elements $A_{J'}$ can be calculated by using effective quadrupole-quadrupole $Q \cdot Q$ or surface delta (SDI) interactions [12]. These two interactions generate level schemes with distinctive features. Thus, for example, the SDI interaction which preserves [13] the seniority quantum number v leads to $9/2^+$ ground state. Contrary to it, the $Q \cdot Q$ interaction does not preserve seniority and leads to $7/2^+$ ground state.

The experimental data, shown in Figure 2, seems to show a transition between these two regimes. In ^{97}Ag, and the neighbouring two isotopes, the $9/2^+$ state is indeed the lowest lying positive-parity state. From ^{103}Ag on, however, the $9/2^+$ and $7/2^+$ states swap their places in accordance with the $Q \cdot Q$ interaction. $7/2^+$ state is the lowest lying state until ^{125}Ag, where the two states are expected to swap their ordering where the seniority scheme would be eventually restored. If so, the $^{129}_{47}\mathrm{Ag}_{82}$ will have the typical seniority scheme shown in Figure 3. It has to be noted that ^{129}Ag excited levels are not observed yet and any deviation from the $\pi g^{-3}_{9/2}$ pattern, that would be experimentally detected, would indicate deviation from the "classical" shell structure.

The smooth transition from SDI- to $Q \cdot Q$-like regimes, observed in the experimental level energies of odd-mass silver nuclei, has been well reproduced by j^{-3} calculations [5], with $A_{J'}$ parametrized with respect to the neighbouring cadmium nuclei. Detailed j^{-3} calculations for the neutron mid-shell ^{113}Ag describe well the low-energy spectrum, and indeed has a a typical seniority broken level structure.

It should be noted, however, that these calculations smear the effect of the neutron component through the two-body terms calculated from the neighbour-

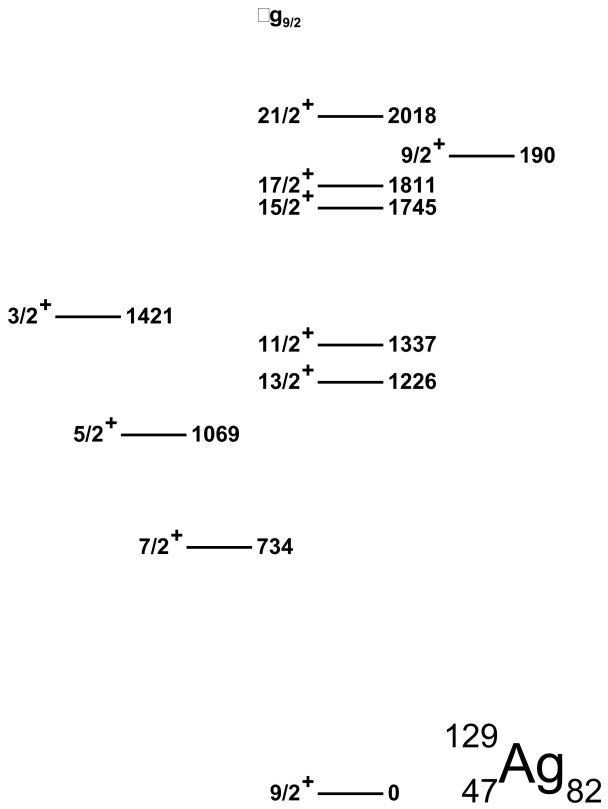

Figure 3. $\pi g_{9/2}^{-3}$ theoretical predictions for $^{129}_{47}\mathrm{Ag}_{66}$. The two-body $A_{J'} = \{0, 1325, 1864, 1992, 2130\}$ keV matrix elements are estimated from $^{130}_{48}\mathrm{Cd}_{82}$.

ing cadmium nuclei. Another downside of this approach is its incapability to explain the $M1$ transitions observed between the members of the same j^{-3} multiplet [9]. As a consequence, large-space Shell model calculations were carried out for $^{123-129}$Ag [5]. They were performed by taking into account both the proton $\pi 1f_{5/2}$, $\pi 2p_{3/2}$, $\pi 2p_{1/2}$, $\pi 1g_{9/2}$ and the neutron $\nu 1g_{7/2}$, $\nu 2d_{5/2}$, $\nu 2d_{3/2}$, $\nu 3s_{1/2}$, and $\nu 1h_{11/2}$ single-particle orbits. The modern jj45pna effective interaction, parametrized with respect to the $A = 132$ nuclei, was used. As a result, more complex wave function were obtained, but the overall result was worse than that obtained from the three-single-j particles calculations. Nevertheless, these calculations had also shown that the $\pi g_{9/2}^{-3}$ configuration plays an important role in the formation of the positive-parity states in the silver nuclei away from the magic numbers.

Recently, truncated large-scale shell model calculations were performed and compared to two-orbit shell model calculations, where only $\pi g_{9/2}^{-3} \otimes \nu h_{11/2}^{m}$

configurations were taken into account [6]. They show a better description of the positive-parity yrast states in ^{113,119,121}Ag isotopes, emphasizing the role of the $\nu h_{11/2}$ intruder orbit in the nature of the positive-parity yrast states in Ag isotopes.

3 Particle(s)–Core Models

A different approach has been exploited in the 1970s [14] within a model based on vibrational field interacting with a cluster of three valence particles or holes. The model succeed in describing large set of states. The magnitude of the $(j, j-1)$ splitting is strongly dependent on the the cluster-core interaction strength and the $j-1$ anomaly has been found to emerge at large values of the interaction parameter.

Further, in the 1970s, Axially-Symmetric-Rotor-plus-Particle Model and Triaxial-Rotor-plus-Particle Model calculations were performed. Examples are presented in Refs [15] and [16]. Within those models, the $j-1$ anomaly is explained via a particle-deformed core interaction and triaxiallity.

More recently, the structure of the mid-shell nuclei ^{111,113}Ag was studied within the Interacting Boson-Fermion Model [18].

The underlying success of those collective models lies in the fact that the valence space of the neutron mid-shell silver nuclei is much larger and quadrupole deformation is well developed.

4 Experimental Data

Systematics of the low-lying positive-parity states in the Ag isotopic chain is presented in Figure 2. It shows two overall distinctive regimes. In the light nuclei, placed close to the $N = 50$ magic number, $7/2^+$ appears above the $9/2^+$ state. There, the respective core energy is ≈ 1000 keV. When approaching the neutron mid shell, however, the core 2^+ level energy decreases to 300-600 keV. As a result, the $9/2^+$ and $7/2^+$ states swap their places, and $7/2^+$ becomes the lowest-lying positive parity state in the silver odd mass nuclei. Thus, the position and the ordering of the $7/2^+$ and $9/2^+$ states are strongly correlated with the 2^+ level energy of the core. This is even more prominent in Figure 4 where, on the left hand side, the $\Delta E = E_{7/2^+} - E_{9/2^+}$ level energy difference is plotted as a function of the core's E_{2^+}. A similar study was performed for the $N = 47$ isotones [17, 18] and was found to follow the same trend.

In the $N = 47$ isotonic chain, at low energies, the level schemes are also dominated by positive-parity states arising from $\nu g_{9/2}$ intruder orbit. Again, when the proton number is close to $Z = 50$, the $9/2^+$ level is the lowest-lying positive-parity state. In those nuclei the $7/2^+$ state is lying at higher energies. The precise $9/2^+$ and $7/2^+$ level energies are listed in Table 2 and compared to the 2^+ level energies of the $N = 48$ nuclei. Deeper in the proton shell, when

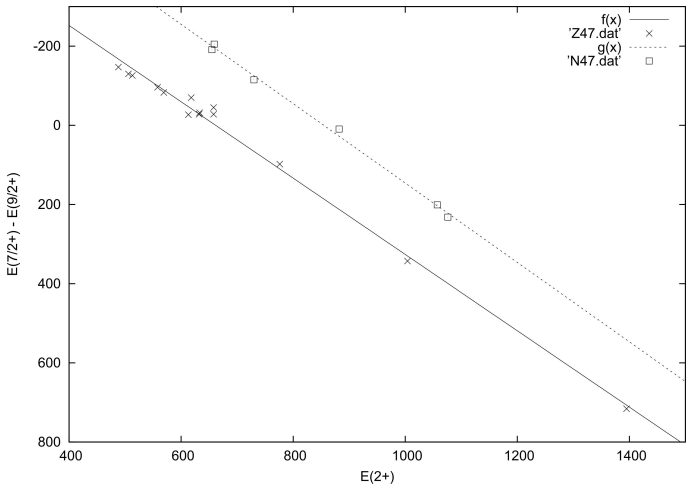

Figure 4. Systematics of $Z = 47$ and $N = 47$ data.

the deformation start to emerge, the two levels swap their places as it is in the $Z = 47$ case.

Thus, at first glance, depending on the relative position with respect to the shell gaps, two excitation patterns can be distinguished. A j^{-3} seniority scheme that can explain the behavior of the nuclei placed close to the shell edges, and a "seniority-broken" regime represented by a different level ordering. Thus, in the nuclei for which one of the two components (protons or neutrons) is close to the magic number and the other is far away from the nearest shell gap, represent excitation features close to the phenomenological j^{-3} configuration with $Q \cdot Q$ interaction, and/or collective-particle(s) model description. The experimental

Table 2. Experimental data for $Z = 47$ and $N = 47$ nuclei and their respective Cd and $N = 48$ cores. Each odd-mass $A-1$ nucleus is considered to have an A mass core. E_{2+} is the first 2^+ level energy. $\Delta = E_{7/2_1^+} - E9/2_1^+$ is calculated from the $7/2_1^+$ and $9/2_1^+$ level energy difference. All energies are given in keV.

				$\boldsymbol{Z = 47,\ 48}$				
E_{2^+}:	1395	1004	776	658	632	633	658	618
Δ:	716	343	98	-28	-28	-32	-45	-70
E_{2^+}:	558	513	488	506	569	613		
Δ:	-96	-126	-147	-130	-83	-27		
				$\boldsymbol{N = 47,\ 48}$				
E_{2^+}:	1057	1076	882	655	659	730		
Δ:	201	232	9.4	-191	-205	-115		

data shown in Figure 2, however, seems to support a more gradual change between these two "orthogonal" regimes.

Nevertheless, what emerges from the systematics in the present study is that the $j, j-1$ splitting strongly depends on the core's 2^+ level energy, suggesting that the core excitation plays an important role already at low excitation energies throughout the entire silver isotopic chain. Similar trend is also observed for the nuclei with three neutron holes below $N = 50$.

Table 3. Experimental data for $Z = 25$ and $N = 25$ nuclei and their respective $Z = 26$ and $N = 26$ cores, respectively. Each odd-mass $A-1$ nucleus is considered to have an A mass core. E_{2+} is the first 2^+ level energy. $\Delta = E_{7/2_1^-} - E9/2_1^-$ is calculated from the $7/2_1^-$ and $9/2_1^-$ level energy difference. All energies are given in keV.

				$\boldsymbol{Z = 25,\ 26}$				
E_{2+}:	764	849	1408	847	811	824	877	746
Δ:	-261	-237	378	-126	-83	-112	-157	-248
				$\boldsymbol{N = 25,\ 26}$				
E_{2+}:	903	1158	1346	984	783	849	1392	
Δ:	-449	-201	174	-159	-272	-253	320	

Similar pattern has been observed in the $Z = 25$ isotopic and $N = 25$ isotonic chains with three valence holes to the proton or neutron magic number 28. There, the higher-j, unique-parity single-particle orbit is f7/2. Nuclear level energies of the odd-mass systems and the respective even-even cores are given in Table 3. In Figure 5 the $7/2^+, 9/2^+$ energy splitting is plotted against the core's 2^+ level energy.

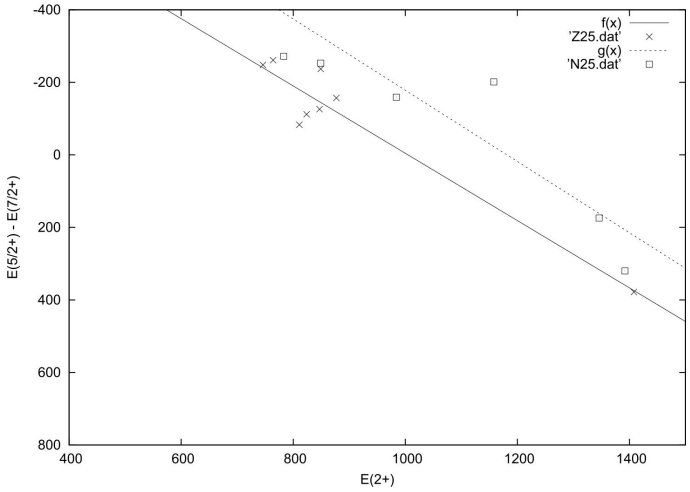

Figure 5. Systematics of $Z = 25$ and $N = 25$ data.

Table 4. Experimental data for $Z = 79$ nuclei and their respective Hg cores. Each odd-mass $A-1$ nucleus is considered to have an A mass core. E_{2^+} is the first 2^+ level energy. $\Delta = E_{7/2^-_1} - E9/2^-_1$ is calculated from the $7/2^-_1$ and $9/2^-_1$ level energy difference. All energies are given in keV.

				$Z = 79,\ 80$				
E_{2^+}:	367	405	413	416	422	428	426	411
Δ:	-219	-215	-127	76	274	500	576	539

In the upper $Z = 50$–82 shell, pure j^{-3} three-particle systems can arise from $\pi h_{11/2}$ single-particle orbit. These can be expected to occur in the $Z = 79$ gold nuclei. Level energy differences have been obtained from the first excited $7/2^-$ and $9/2^-$ states and plotted in Figure 6 versus 2^+ level energies of the core mercury nuclei. In this mass region, however, the correlation is broken which is probably due to the larger valence space leading to more mixed wave functions.

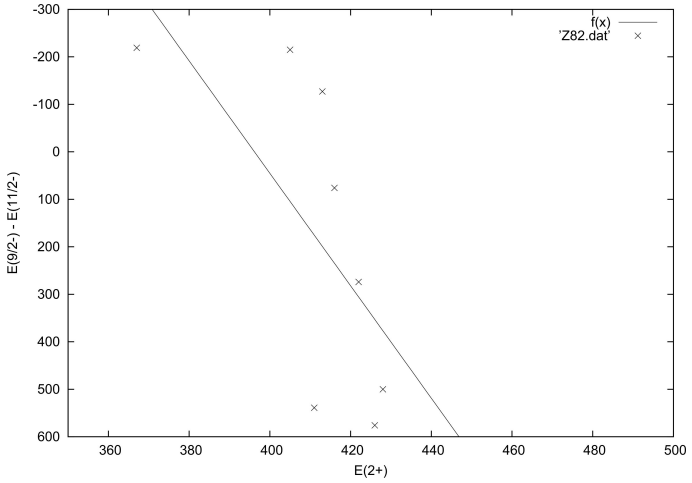

Figure 6. Systematics of $Z = 79$.

5 Conclusion

The Nuclear Shell model and the Particle-Core models are among the cornerstones in the modern Nuclear physics. Their success is based on the applicability of the adiabatic principle which allows to disentangle single-particle from collective modes. Thus, nuclei of well pronounced shell-model behaviour are located near the magic numbers, while nuclei with a large number of valence particles form the regions of collectivity on the Segré chart. In each of these regimes, however, there are distinctive features that are outside the respective model valence space, but rather reside in the "adversary" group of models. Such

a feature is the seniority concept, which is well within the spherical shell model space, but it is completely "orthogonal" to the deformed shell model concept. The data on the light and medium-mass systems, however, seems to support a gradual evolution between the two regimes, that can be tracked by using the low-lying yrast states in the three-holes isotopic and isotonic chains, respectively. In the heavy-mass nuclei the correlation between the 7/2 and 9/2 components of the j^{-3} multiplet is broken.

Acknowledgements

This study is supported by the Bulgarian National Science Fund under contract DFNI-E02/6

References

[1] M.G. Mayer, *Phys. Rev.* **74** (1948) 235.
[2] O. Haxel, J.H.D. Jensen, H.E. Suess, *Phys. Rev.* **75** (1949) 1766.
[3] M.G. Mayer, *Phys. Rev.* **78** (1950) 16.
[4] K.L.G. Heyde, *The Nuclear Shell model* (Springer-Verlag, 1994).
[5] S. Lalkovski et al., *Phys. Rev. C* **87** (2013) 034308.
[6] Y.H. Kim et al., *Phys. Lett. B* **772** (2017) 403.
[7] S. Lalkovski et al., *Phys. Rev. C* **96** (2017) 044328.
[8] L.S. Kisslinger, *Nucl. Phys.* **78** (1966) 341.
[9] P. Van Isacker, private communications.
[10] I.M. Band, and Yu.I. Kharitonov, *At. Data Nucl. Data Tables* **10** (1971) 107.
[11] M. Lipoglavsek, et al., *Phys. Rev. C* **72** (2005) 061304(R).
[12] A. Escuderos, and L. Zamick, *Phys. Rev. C* **73** (2006) 044302.
[13] P. Van Isacker, and S. Heinze, *Ann. Phys.* **349** (2014) 73.
[14] V. Paar, *Nucl. Phys. A* **211** (1973) 29.
[15] V. Popli, et al. *Phys. Rev. C* **20** (1979) 1350.
[16] A.W.B. Kolshoven et al., *Nucl. Phys. A* **315** (1979) 334.
[17] S. Lalkovski, *Nuclear Theory* **36** (2017) 254.
[18] S. Lalkovski, *Bulg. J. Phys.* **44** (2017) 499.